The GDP-dependent Rab27a effector coronin 3 controls endocytosis of secretory membrane in insulin-secreting cell lines

Toshihide Kimura[1], Yukiko Kaneko[1], Shogo Yamada[1], Hisamitsu Ishihara[2], Takao Senda[3], Akihiro Iwamatsu[4] and Ichiro Niki[1,*]

[1]Department of Pharmacology, Oita University Faculty of Medicine, 1-1 Idaigaoka, Hasama, Yufu, Oita 879-5593, Japan
[2]Division of Molecular Metabolism and Diabetes, Tohoku University Graduate School of Medicine, 2-1 Seiryo, Aoba, Sendai, Miyagi 980-8575, Japan
[3]Department of Anatomy I, Fujita Health University School of Medicine, Toyoake, Aichi 470-1192, Japan
[4]Protein Research Network, Inc., 1-13-5 Fukuura, Kanazawa-ku, Yokohama 236-0004, Japan
*Author for correspondence (e-mail: niki@med.oita-u.ac.jp)

Accepted 2 July 2008
Journal of Cell Science 121, 3092-3098 Published by The Company of Biologists 2008
doi:10.1242/jcs.030544

Summary

Rab27a is involved in the control of membrane traffic, a crucial step in the regulated secretion. Typically, the guanosine triphosphate (GTP)-bound form has been considered to be active and, therefore, searching for proteins binding to the GTP-form has been attempted to look for their effectors. Here, we have identified the actin-bundling protein coronin 3 as a novel Rab27a effector that paradoxically bound guanosine diphosphate (GDP)-Rab27a in the pancreatic β-cell line MIN6. Coronin 3 directly bound GDP-Rab27a through its β-propeller structure. The most important insulin secretagogue glucose promptly shifted Rab27a from the GTP- to GDP-bound form. Knockdown of coronin 3 by RNAi resulted in the inhibition of phogrin (an insulin-granule-associated protein) internalization and the uptake of FM4-64 (a marker of endocytosis). Similar results were reproduced by disruption of the coronin-3–GDP-Rab27a interaction with the dominant-negative coronin 3, and coexpression of the GDP-Rab27a mutant rescued these changes. Taken together, our results indicate that interaction of GDP-Rab27a and coronin 3 is important in stimulus-endocytosis coupling, and that GTP- and GDP- Rab27a regulates insulin membrane recycling at the distinct stages.

Supplementary material available online at
http://jcs.biologists.org/cgi/content/full/121/18/3092/DC1

Key words: Rab27a, Coronin 3, Endocytosis, Insulin, GDP-dependent effector

Introduction

The secretory process comprises pre-exocytotic stages (granule synthesis, anterograde transport, docking and post-docking), exocytosis and post-exocytotic stages, including membrane endocytosis and retrograde transport. Membrane trafficking is crucial for the regulation of the size of the readily releasable pool of the secretory granules and for the recovery of the granule membranes (Niki et al., 2003). Although many proteins participating in membrane trafficking have been found, knowledge about regulatory mechanisms is still limited.

The small guanosine triphosphatase (GTPase) superfamily, comprising the Ras, Rho, Rab, Ran and Arf subfamilies, regulates various cellular functions including regulated secretion (Takai et al., 2001; Wennerberg et al., 2005). They bind either GTP or GDP, and form a molecular switch through interaction with their specific effectors. Conventionally, the GTP-bound form is regarded as active and, therefore, searching for proteins binding the GTP-form has been attempted to look for their effectors.

Rab27a is a member of the Rab family that is involved in the control of membrane traffic (Zerial and McBride, 2001). Its mutation causes a human genetic disease, the Griscelli syndrome, which is characterized by immunodeficiency and pigment dilution in hair (Menasche et al., 2000; Pastural et al., 2000). Rab27a regulates secretion of lytic granules in cytotoxic T lymphocytes and intracellular transport of melanosomes in melanocytes (Bahadoran et al., 2001; Haddad et al., 2001; Hume et al., 2001; Kuroda and Fukuda, 2004; Menasche et al., 2000; Stinchcombe et al., 2001; Wilson et al., 2000). Ashen mice with natural mutation in *Rab27a* show glucose intolerance with decreased insulin secretion (Kasai et al., 2005; Wilson et al., 2000). Therefore, Rab27a has been proposed to regulate insulin secretion. Indeed, Noc2 (also known as RPH3L) and Slp4 (also known as granuphillin-a or SYTL4) by their interaction with Rab27a regulate intracellular traffic of the insulin granules (Cheviet et al., 2004; Kotake et al., 1997; Torii et al., 2002; Wang et al., 1999; Yi et al., 2002). Another Rab27a effector, MYRIP (also known as Slac2-c) might mediate interaction between insulin granules and cortical actin (Waselle et al., 2003). All known Rab27a effectors bind GTP-Rab27a (Fukuda, 2005).

In this study, we tried to find a new Rab27a effector protein by proteomic analysis to investigate the underlying mechanism of membrane traffic in the β cell. We eventually identified coronin 3 as a novel effector, which paradoxically binds Rab27a in a GDP-dependent manner. We also found interaction of Rab27a with coronin 3 regulates endocytosis of the insulin granule membranes. Here, we suggest that both GTP- and GDP-forms of Rab27a control membrane traffic of the insulin granules at distinct stages.

Results

Identification of coronin 3 as a GDP-bound Rab27a-interacting protein

Extracts from the insulin-secreting β-cell line MIN6 were applied to a GDP-Rab27a-affinity column to investigate GDP-Rab27a-interacting proteins. Specific binding proteins were analyzed by silver staining. A protein with the molecular weight (M_r) of 53,000 (p53) bound GDP-Rab27a, but not glutathione S-transferase (GST) alone (Fig. 1A). We identified p53 as coronin 3 by peptide-mass fingerprinting (supplementary material Fig. S1) and immunoblotting (Fig. 1B). A co-immunoprecipitation assay with MIN6 extracts confirmed that coronin 3 endogenously interacts with Rab27a (Fig. 1C). Intracellular distribution of Rab27a and coronin 3 in the mouse pancreatic islet was examined by immunohistochemical analysis (Fig. 1D,E). Both Rab27a and coronin 3 were preferentially expressed in the mouse islet cells including the insulin-positive β cells (Fig. 1D,E).

Interaction of coronin 3 with GDP-Rab27a

Guanine-nucleotide specificity of the interaction between coronin 3 and Rab27a was determined by a co-transfection assay in COS-7 cells. Immunoblot analysis revealed that Rab27a-T23N, a mutant mimicking GDP-Rab27a, co-immunoprecipitated with coronin 3, but that Rab27a-Q78L, a GTP-Rab27a mutant, did not (Fig. 2A, upper panel). Furthermore, coronin 3 was reciprocally co-immunoprecipitated with only Rab27a-T23N (supplementary material Fig. S2A). By contrast, Rab27a-Q78L was co-immunoprecipitated with the synaptotagmin-like protein-homology domain (SHD) that is the GTP-Rab27a-binding domain of its specific effectors (Kondo et al., 2006), indicating that coronin 3 specifically binds Rab27a in a GDP-dependent manner (Fig. 2A, lower panel). The GDP-bound form of Rab3a, which has the highest homology with Rab27a (40% similarity on the amino acid level), also co-immunoprecipitated with coronin 3 (supplementary material Fig. S2B). However, the binding efficiency was considerably lower (supplementary material Fig. S2C). By contrast, the GDP-bound form of Rab5a was not immunoprecipitated together with coronin 3 (supplementary material Fig. S2C). Among coronin isoforms, coronin 2, another ubiquitous isoform of coronin, also interacted with Rab27a in MIN6 cells (supplementary material Fig. S2D) and the binding was, again, GDP-dependent (supplementary material Fig. S2E). Coronin 1, coronin 4 and coronin 5 were not expressed in the pancreas (Nakamura et al., 1999). To examine the direct interaction between Rab27a and coronin 3, an in-vitro-binding assay was performed using wild-type (WT) Rab27a and its mutants. Purified FLAG-tagged coronin 3 was incubated with glutathione-beads conjugated with GST, with GST-Rab27a-WT charged using the non-hydrolysable GTP analogue GTPγS or GDP, or with the GST-Rab27a mutants. Coronin 3 directly bound GDP-charged Rab27a WT and Rab27a-T23N (Fig. 2B). Next, we determined the binding site of coronin 3 to Rab27a by co-transfection assay in COS-7 cells. FLAG-Rab27a-T23N and green fluorescent protein (GFP)-tagged various deletion mutants of coronin 3 were co-transfected into COS-7 cells, and their binding was evaluated by immunoprecipitation (Fig. 2C). Rab27a-T23N bound coronin-3-WT (amino acids 1-474), coronin-3-N (1-71), coronin-3-WD (72-314, containing the tryptophan and aspartate repeat), and coronin-3-ΔC (1-314) but not GFP and coronin-3-C (315-474), which is responsible for the actin binding (Spoerl et al., 2002) (Fig. 2C). Therefore, residues 1-314 of coronin 3, which form the β-propeller structure for protein-protein interactions (Appleton et al., 2006),

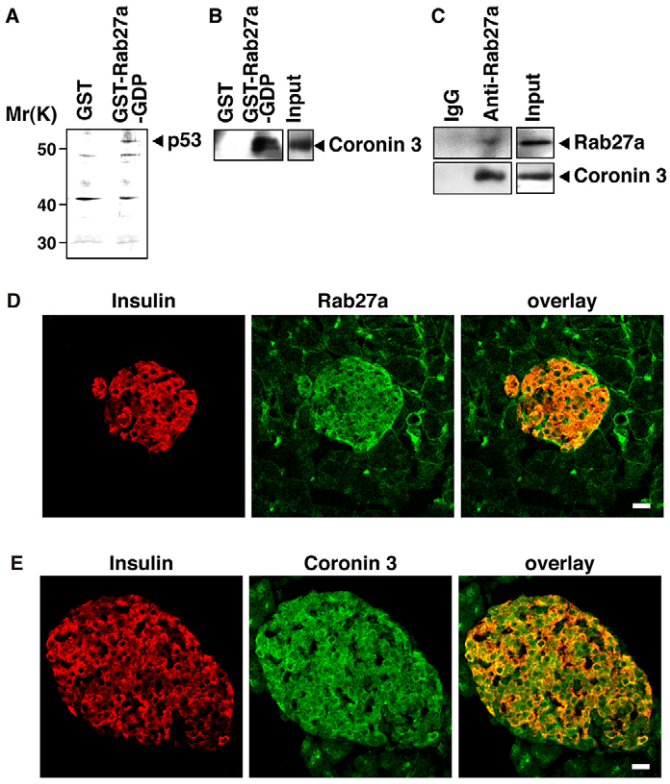

Fig. 1. Identification of coronin 3 as a GDP-Rab27a-interacting protein in pancreatic β cells. (A,B) Eluates from affinity columns were analyzed by silver staining (A) and immunoblotting with anti-coronin 3 antibody (B). (C) Immunoprecipitation of MIN6 extracts using anti-Rab27a antibody and immunoblotting using anti-Rab27a and anti-coronin 3 antibodies. 0.2% of the input protein was co-immunoprecipitated. (D,E) Mouse pancreata were double-stained using anti-insulin antibody and anti-Rab27a antibody (D) or anti-coronin 3 antibody (E). Scale bars, 20 μm.

are essential for the binding to GDP-Rab27a. Rab27a-T23N preferentially interacted with coronin-3-N, coronin-3-WD, and coronin-3ΔC compared with coronin-3-WT, probably because Rab27a binding might be hindered by the C-terminus of coronin 3, which intramolecularly binds the N-terminus (Spoerl et al., 2002).

The binding constant and stoichiometry between coronin 3 and Rab27a-T23N were determined using the same assay that is described for Fig. 2B. The dissociation constant (K_d), as determined by Scatchard analysis, was 0.2 μM and the stoichiometry was ~0.01 (Fig. 2D). The binding affinity of coronin 3 to Rab27a-T23N was ~20 times higher than that to Rab3a-T36N (4.2 μM) (supplementary material Fig. S2F). This result is consistent with the results from the co-immunoprecipitation experiments (supplementary material Fig. S2C). The stoichiometry value was relatively low under this condition, possibly because not all Rab27a-T23N formed the stable complex with GDP. We consider that the stoichiometry value in vivo may be higher than this value (Fig. 2C).

We examined whether glucose, the most important insulin secretagogue, alters the extent of GDP or GTP-bound forms of Rab27a in MIN6 cells by GTP- and GDP-Rab27a pull-down assays. GST-SHD efficiently bound T7-Rab27a-Q78L as previously reported (Kondo et al., 2006) and GST–coronin-3-ΔC only bound T7-Rab27a-T23N, indicating that SHD and coronin-3-ΔC specifically bind GTP- and GDP-Rab27a, respectively (Fig. 2E). Next, we quantified GTP- and GDP-Rab27a in glucose-stimulated

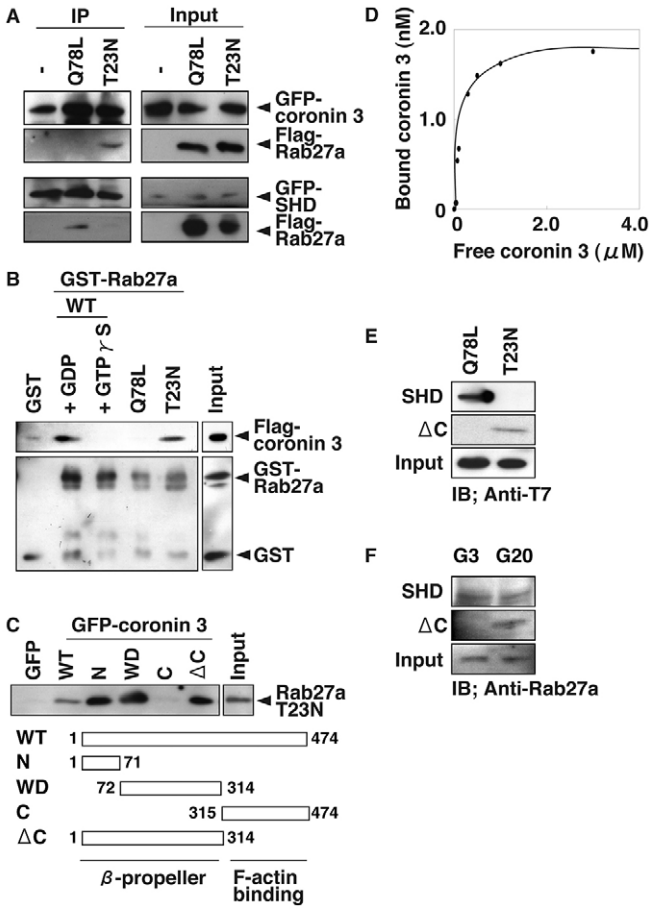

Fig. 2. Coronin 3 binds glucose-induced GDP-Rab27a through the β-propeller structure. (A) Immunoprecipitation of COS-7 extracts that express FLAG-Rab27a mutants and GFP-coronin 3 (upper panel) or GFP-SHD (lower panel) using anti-GFP antibody, and immunoblotting using anti-GFP and anti-FLAG antibodies. 0.2% of the input protein was co-immunoprecipitated. (B) In-vitro-binding assay of purified FLAG-coronin 3 and Rab27a mutants and immunoblotting using anti-FLAG and anti-GST antibodies. (C) Immunoprecipitation of COS-7 extracts that express FLAG-Rab27a-T23N and GFP-coronin 3 deletion mutants using anti-GFP antibody, and immunoblotting using anti-FLAG antibody. 2.0% of the input protein was co-immunoprecipitated except for WT (0.2%). (D) The indicated concentrations of MBP–coronin-3-ΔC were incubated with beads conjugated to GST-Rab27a-T23N; the K_d value was calculated using Scatchard analysis. (E) COS7 lysates that express T7-Rab27a mutants were incubated with beads conjugated to GST-SHD or GST-coronin-3-ΔC. The bound proteins were analyzed by immunoblotting using anti-T7 antibody. (F) MIN6 cells stimulated with 20 mM glucose were extracted and incubated with beads conjugated to GST-SHD or GST-coronin-3-ΔC. The bound proteins were analyzed by immunoblotting using anti-Rab27a antibody.

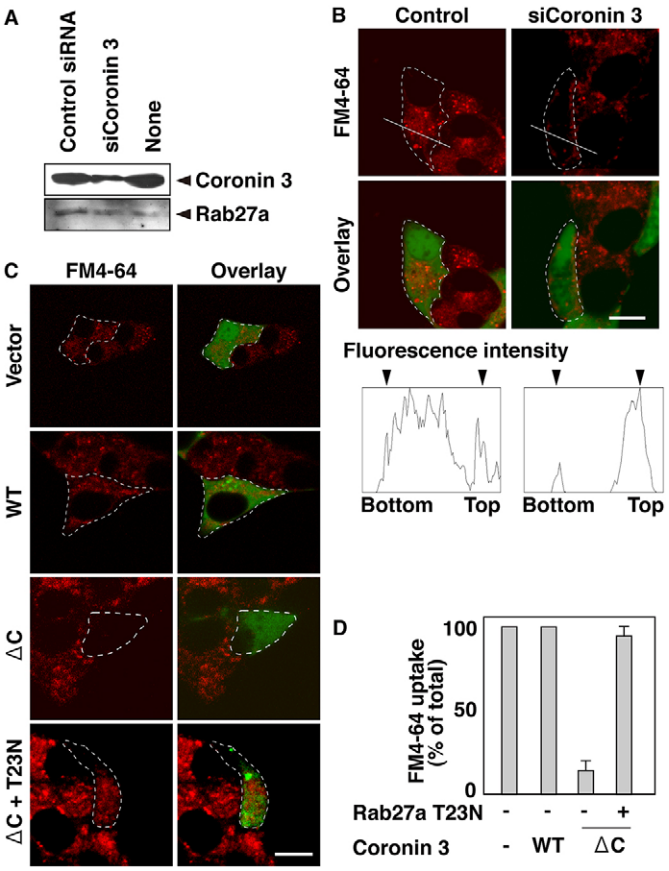

Fig. 3. The interaction between GDP-Rab27a and coronin 3 is essential for endocytosis. (A) Coronin-3-silenced MIN6 cells were analyzed by immunoblotting with anti-coronin 3 and anti-Rab27a antibodies. (B) Coronin-3-silenced MIN6 cells that express GFP (green in overlay) as a transfection marker were labeled with FM4-64 (top panel, and red in overlay). Fluorescence intensity of FM4-64 on the line is shown in lower panels. Scale bar, 10 μm. (C) GFP-coronin three mutants expressing MIN6 cells were labeled with FM4-64. For rescue experiments, T7-Rab27a-T23N was co-transfected. Dashed outlines indicate transfected cells. Scale bar, 10 μm. (D) Fluorescence intensity of FM4-64 was analyzed. Among the transfected cells, the rate of cells with cytoplasmic distribution of fluorescence is given presented as a percentage. More than 40 randomly selected cells (more than ten cells per experiment) were examined. Data are expressed as the mean ± s.d. from four independent experiments. All the experiments were carried out in the presence of 25 mM glucose.

and unstimulated MIN6 cells. Stimulation with 20 mM glucose for 2 minutes slightly decreased GTP-Rab27a and increased GDP-Rab27a without changing the total amounts (Fig. 2F). These results indicate that Rab27a in unstimulated MIN6 cells mostly binds GTP and that glucose stimulation converts GTP-Rab27a to its GDP-bound form. Thus, GTP hydrolysis on Rab27a might be activated upon glucose stimulation.

Coronin 3 regulates the endocytosis

It has been suggested that the coronin family regulates membrane internalization through actin remodeling (Uetrecht and Bear, 2006). Thus, we investigated whether coronin 3 controls endocytosis in pancreatic β cells. We used glucose (25 mM) in culture medium as the stimulant for exocytosis and endocytosis in this set of experiments. In RNA interference (RNAi) experiments, immunoblot analysis showed the decrease in coronin 3 expression after 24 hours treatment with coronin 3 small interfering RNA (siRNA) (Fig. 3A). siRNA targeting coronin 3 did not affect cell viability and Rab27a expression (Fig. 3A). Coronin-3-silenced MIN6 cells expressing GFP as a transfection marker were labeled with the red lipidic styryl dye FM4-64. A previous report has shown that FM4-64 labeled vesicles colocalized with endobrevin and that the probe could visualize vesicle recycling in MIN6 cells (Nagamatsu et al., 2001). FM4-64 fluorescence in control cells was mainly localized in cytosolic vesicles, showing a characteristic punctate pattern (Taraska and Almers, 2004) (Fig. 3B). By contrast, the uptake of FM4-64 fluorescence was inhibited in coronin-3-silenced cells (Fig. 3B)

suggesting that coronin 3 regulates endocytosis. In cells expressing GFP– or GFP–coronin-3-WT, FM4-64 fluorescence was dominantly localized in cytosolic vesicles (Fig. 3C). By contrast, FM4-64 uptake was inhibited in cells expressing GFP-fused dominant-negative coronin-3-ΔC, which bound GDP-Rab27a (Fig. 2C) without actin-bundling activity (Spoerl et al., 2002) (Fig. 3C). The inhibition of FM4-64 uptake by coronin-3-ΔC was rescued by co-transfection of Rab27a-T23N (Fig. 3C,D). The dominant-negative coronin 3 mutant prevented endocytosis because it inhibited endogenous GDP-Rab27a–coronin-3 binding and eventual actin remodeling that is essential for endocytosis (Schafer, 2002). The rescue of the effects of coronin-3-ΔC by expression of the Rab27a-T23N was owing to sequestration of coronin-3-ΔC. This treatment enabled endogenous coronin 3 to interact with endogenous GDP-Rab27a, and endocytosis was eventually rescued, possibly via its effect on actin network. Taken together, these findings suggest that the interaction between coronin 3 and GDP-Rab27a is necessary for endocytosis in the pancreatic β cell.

Coronin 3 regulates the internalization of phogrin, a membrane protein associated with insulin granules

To clarify whether the interaction between coronin 3 and GDP-Rab27a has a role in the internalization of the membrane of insulin granules, phogrin-GFP was introduced in living MIN6 cells. Phogrin, an integral membrane protein, closely colocalizes with insulin granules (Pouli et al., 1998). Phogrin-GFP showed a punctate pattern similar to that of insulin in control cells (Fig. 4A). By contrast, phogrin-GFP was mainly present near the plasma membrane in coronin-3-silenced cells (Fig. 4A). It has been reported that, after exocytosis, phogrin is internalized into small vesicles that recycle to an insulin-containing compartment for a subsequent round of exocytosis (Vo et al., 2004). To determine whether the internalization of phogrin is regulated by the interaction between GDP-Rab27a and coronin 3, *Discosoma* red fluorescent protein (DsRed)–coronin-3 or its mutants, and phogrin-GFP were co-transfected into MIN6 cells. DsRed–coronin-3-WT was partly colocalized with phogrin-GFP and had no effect on the localization of phogrin-GFP (Fig. 4B). In MIN6 cells expressing DsRed–coronin-3-ΔC, most phogrin-GFP was present near the plasma membrane (Fig. 4B). This is due to the inhibition of phogrin internalization, because anti-phogrin antibodies against the extracellular domain were not taken up and showed similar peripheral distribution in coronin-3-ΔC-expressing cells (supplementary material Fig. S3). The inhibition of phogrin-GFP internalization by coronin-3-ΔC was, again, rescued by its co-transfection of Rab27a-T23N (Fig. 4B,C). Taken together, these results indicate that glucose induces conversion of Rab27a from the GTP- to GDP-bound form and the formation of the GDP-Rab27a-coronin 3 complexes, resulting in internalization of membranes of insulin granules in the β cell.

Discussion

As shown previously, GTP-Rab27a functions at pre-exocytotic stages through interaction with its GTP-dependent effectors, such as Slp4 (Fukuda, 2005; Izumi et al., 2003). We consider that the GTP-dependent Rab27a actions preferentially take place under basal conditions in order to expand the size of the readily releasable pool of insulin granules. Our present results indicate that GDP-Rab27a also has a crucial role in the control of endocytosis of the insulin granules. The target protein is coronin 3, an actin-bundling protein (Hasse et al., 2005; Iizaka et al., 2000; Rosentreter et al., 2007;

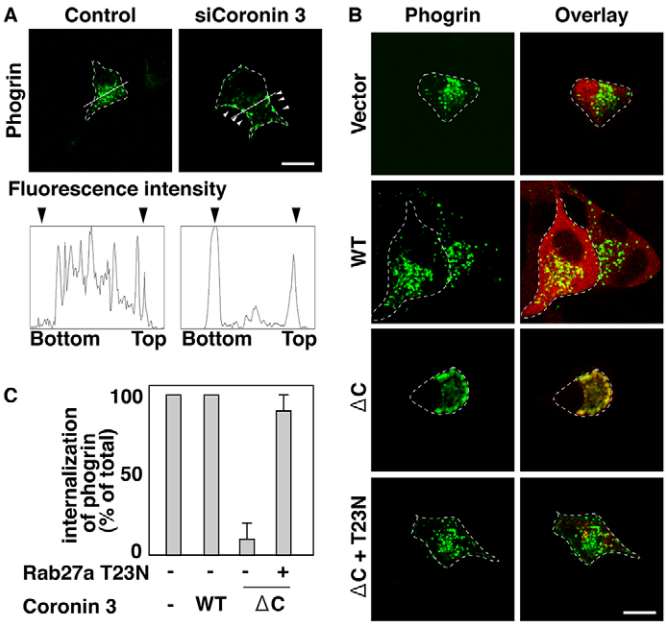

Fig. 4. The interaction between GDP-Rab27a and coronin 3 is essential for internalization of phogrin. (A) Coronin 3 siRNA was co-transfected with phogrin-GFP into MIN6 cells. GFP-positive cells were regarded as coronin-3-silenced cells. Arrowheads denote phogrin-GFP localized in the cell periphery. Fluorescence intensity of phogrin-GFP on the line is shown in lower panels. Scale bar, 10 μm. (B) MIN6 cells expressing DsRed-coronin 3 mutant and phogrin-GFP were evaluated. For rescue experiments, T7-Rab27a-T23N was co-transfected. Dashed outlines indicate transfected cells. Scale bar, 10 μm. (C) Fluorescence intensity was analyzed in the same way as in Fig. 3D. All experiments were carried out in the presence of 25 mM glucose.

Spoerl et al., 2002). Since glucose shifted Rab27a from the GTP- to GDP-form, we propose a model where Rab27a is a pivotal protein in stimulus-endocytosis coupling in pancreatic β cells, and a key molecule for membrane recycling of the insulin granules (Fig. 5).

The effects of coronin 3 on endocytosis might involve a mechanism other than its direct action on actin bundling. Coronin1 is purified together with the complex of the actin-related proteins 2 and 3 (Arp2/3) (Machesky et al., 1997), and this interaction is confirmed by studies on yeast coronin (Humphries et al., 2002). Yeast coronin directly binds the Arp2/3 complex through the C-terminal region and regulates activity of Arp2/3 on actin nucleation. Recently, high-speed video microscopy demonstrated that yeast coronin is one regulator of the Arp2/3-regulated endocytic actin patch (Galletta et al., 2008). Coronin 3 also interacts with the Arp2/3 complex (Rosentreter et al., 2007). By analogy with yeast coronin, the C-terminal region of coronin 3 might be the candidate for Arp2/3-binding site. Inhibition of endocytosis by coronin-3-ΔC and our rescue experiment (Fig. 3C and Fig. 4B) might reflect direct and/or Arp2/3-mediated remodeling of actin. Interaction of coronin 1 or coronin 2 with the Arp2/3 complex is regulated by phosphorylation of the serine residue at position 2 (Ser2) by protein kinase C (PKC), where phosphorylation of Ser2 reduced interaction with Arp2/3 (Cai et al., 2005; Foger et al., 2006). Interestingly, Ser2 is conserved in mammalian coronins except coronin 3 (supplementary material Fig. S1). Therefore, Rab27a may modulate the activity of Arp2/3 via GDP-dependent binding to coronin 3, although this possibility awaits confirmation.

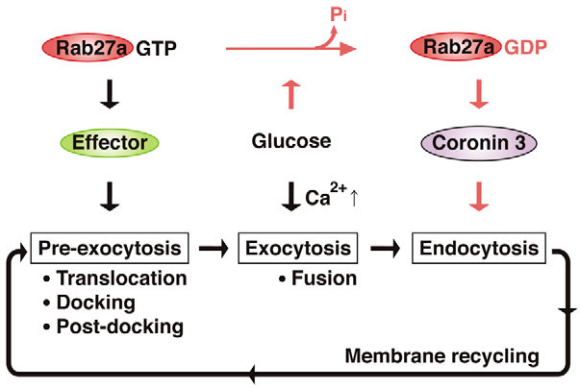

Fig. 5. Schematic model for Rab27a function at membrane traffic. GTP-Rab27a functions at pre-exocytotic stages through interaction with its GTP-dependent effectors under basal conditions. Glucose triggers exocytosis via closure of the ATP-sensitive K^+ channel, opening of the voltage-dependent Ca^{2+} channel and an eventual rise in cytosolic Ca^{2+}. Glucose also causes a shift from GTP-Rab27a to GDP-Rab27a, which regulates endocytosis through interaction with coronin 3. Both GTP- and GDP-bound forms of Rab27a control a series of the insulin granule traffic at the distinct stages.

Interestingly, coronin 3 does not share any common domain with other known GTP-dependent effectors of Rab27 (Kuroda et al., 2002). This suggests the presence of an unknown class of GDP-dependent effectors. To our knowledge, a GDP-dependent effector for any members of the Rab family has only been reported once, in a report showing that GDP-Rab11 interacts with protrudin in PC12 cells (Shirane and Nakayama, 2006). Protrudin possesses a GDP-dissociation inhibitor (GDI) consensus sequence at which it binds Rab11. However, coronin 3 lacks this motif. We expect that identification of GDP-dependent effectors of Rab proteins will reveal unfound molecular mechanisms of pleiotropic actions of Rab GTPases. GDP-Rab27a bound both coronin-3-N (1-71) and coronin-3-WD (72-314) (Fig. 2C). Recent structural studies on coronin (Appleton et al., 2006; Rosentreter et al., 2007) demonstrated that the N-terminal region of coronin forms the first blade (hidden blade) and participate in the seven-bladed β-propeller structure. The blades within the propeller are arranged in a circular fashion around a central axis. Rab27a-T23N should therefore interact with this structure composed of both coronin-3-N and coronin-3-WD.

Rab27a, similar to other small GTPases, has GTP-bound and GDP-bound forms that are interconvertible by GDP-GTP exchange and GTPase reactions. The guanine nucleotide exchange factor (GEF) facilitates the release of GDP from Rab proteins, thereby promoting the binding of GTP. GTPase activating protein (GAP) stimulates the intrinsic GTPase activity of Rab proteins, which subsequently converts Rab to its GDP-bound form. Since glucose promptly caused a shift from GTP- to GDP-Rab27a (Fig. 2F), it should inhibit GEF activity or promote GAP activity to Rab27a. In platelets, Rab27 (isoforms unidentified) is predominantly present in the GTP-bound form in unstimulated platelets, and stimulation with thrombin increases the amount of GDP-Rab27 through the activation of GAP (Kondo et al., 2006). These findings raise the possibility that glucose activates a Rab27a-specific GAP in the β cell. GTP-Rab27a on the insulin granules localizes in the vicinity of the plasma membrane via Slp4 and the plasma membrane-anchored SNARE syntaxin-1a (Gomi et al., 2005). Thus, we consider that the glucose-dependent activation of a Rab27a-specific GAP causes conversion of GTP-Rab27a to GDP-Rab27a in the cell periphery and regulates membrane recycling of the insulin granules. Interestingly, two Tre2-Bud2-Cdc16 (TBC) proteins have recently been identified to function as Rab27a-specific GAPs in melanocytes (Itoh and Fukuda, 2006). Further studies are required to investigate the regulation of Rab27a-specific GAP by glucose in the β cell.

The induction of coronin-3-ΔC inhibited endocytosis of insulin granule membrane (Fig. 4B; supplementary material Fig. S3). Coronin-3-ΔC bound GDP-Rab27a more efficiently than coronin-3-WT (Fig. 2C), thus we consider that coronin-3-ΔC inhibits the GDP-Rab27a-dependent function of native coronin 3 by forming a complex with GDP-Rab27a. In support of this, the inhibition of endocytosis by coronin-3-ΔC was rescued when transfected together with Rab27a-T23N (Fig. 4B). Coronin proteins have a central role in a variety of cellular processes, including intracellular vesicle formation and trafficking by their actin cytoskeleton-related functions (Uetrecht and Bear, 2006). Thus, the F-actin-binding and -bundling activities of coronin 3 will be involved in the coronin-3-mediated endocytosis. In fact, there is growing evidence that F-actin has a direct role in endocytosis (Engqvist-Goldstein and Drubin, 2003). Because coronin-3-ΔC, which does not contain the F-actin binding region, does not have actin-bundling activity (Spoerl et al., 2002) but binds GDP-Rab27a (Fig. 2C), the mutant forms an inactive complex with GDP-Rab27a in the cells. Our data suggest that endocytosis of the membranes of insulin granules is mediated by coronin-3-regulated modulation of actin. Further studies are needed to clarify the correlation between coronin-3-regulated actin dynamics and endocytosis.

Insulin is the most important hormone for glucose homeostasis. Diabetes mellitus is defined as chronic hyperglycemia owing to relative insulin deficiency. Impairment of the secretory activity in β cells is seriously involved in the pathogenesis. In particular, abnormality in glucose-induced insulin release precedes the onset of type 2 diabetes mellitus (Ashcroft and Rorsman, 2004; Kahn, 2001). We, therefore, consider that the present glucose-dependent signaling in the membrane recycling system, as well as the exocytotic pathway may be damaged in this disease. This is the first paper reporting the molecular mechanism of regulated endocytosis of the secretory granule membranes in the β cell.

Materials and Methods

Materials

cDNA encoding mouse Rab27a (MGC-6415) was purchased from ATCC. cDNA encoding rat phogrin was kindly provided by Eji Kawasaki (Nagasaki University, Japan). pFLAG-CMV-2b-Rab3a was kindly provided by Susume Seino (Kobe University, Japan) (Matsumoto et al., 2004). pAcGFP-C1 and pDsRed-Monomer-C1 vectors were purchased from Clontech. pcDNA3.1/Hygro(–) vector, pGEX-4T-1 vector, and pMAL-p4x vector were purchased from Invitrogen, GE Healthcare UK Ltd., and BioLabs, respectively. Anti-phogrin antibody was kindly provided by John C. Hutton (University of Colorado Denver Health Sciences Center, Denver, CO). The following antibodies were used: anti-Rab27a (H-60) polyclonal antibody, anti-FLAG M2 antibody, and anti-GST (GST-2) antibody (Sigma-Aldrich); anti-Rab27a (M02) monoclonal antibody (Abnova); anti-GFP antibody (MBL); anti-T7 antibody (Novagen); anti-coronin-3 (ab15719) antibody (Abcam); anti-coronin-2 (A301-317A) antibody (BETHYL). For antibody production, New Zealand White rabbits were immunized with a synthetic peptide corresponding to the C-terminal amino acids 461-474 of coronin 3, and anti-coronin-3 antibodies were affinity-purified by exposure to antigen-bound Affigel 102 beads (Bio-Rad). Simian-kidney-derived COS-7 cells were obtained from Cell Resource Center for Biomedical Research, Tohoku University. The insulin-secreting β-cell line MIN6 was kindly provided by Jun-Ichi Miyazaki (Osaka University, Japan). This study was approved by the Ethical Committee for Animal Experiments at Oita University (Oita, Japan).

Plasmid constructs

pcDNA-T7 and pcDNA-FLAG were generated by ligation of the fragments coding for the T7 and FLAG epitope tags to the pcDNA3.1/Hygro(–) vector, respectively (Vitour et al., 2004). cDNAs of mouse coronin 2, coronin 3 and Rab5a were amplified by polymerase chain reaction (PCR) from an MIN6 cDNA library. The cDNAs

encoding coronin-3-N (amino acids 1-71), coronin-3-WD (72-314), coronin-3-C (72-474), and coronin-3-ΔC (1-314) were also amplified by PCR. All the DNA point mutations were introduced using Quick Change kit (Strategene,). SHD was generated by PCR using KIAA0624 clone provided by Kazusa DNA Research Institute as template (Kondo et al., 2006). These cDNAs were subcloned into pAcGFP-C1, pDsRed-Monomer-C1 (Clontech), pGEX-4T-1 (Invitrogen), pcDNA-T7, and pcDNA-FLAG. Rat phogrin cDNA was subcloned into pEGFP-N1 (Clontech) (Pouli et al., 1998).

GDP-Rab27a affinity column chromatography

GST or GST-Rab27a at 2 mM was incubated with 250 µl of glutathione-Sepharose 4B beads (GE Healthcare), pre-equilibrated with NE-buffer (20 mM HEPES at pH 7.5, 5 mM $MgCl_2$, 1 mM DTT, 100 mM NaCl, 10 mM EDTA, 10 mM GDP), for 1 hour at 4°C under rotation. The beads were incubated for 30 minutes at room temperature with NE-buffer in the presence of 1 mM GDP and further incubated with NS-buffer (20 mM HEPES at pH 7.5, 5 mM $MgCl_2$, 1 mM DTT, 100 mM NaCl, 1 mM GDP) for 20 minutes at room temperature under rotation. After packing the beads into columns, MIN6 cell membrane fractions were loaded onto the prepared columns, and washed with NS-buffer. The proteins bound to the affinity columns were eluted by NS-buffer containing 1.5 M NaCl. Proteins in the eluates were separated by SDS-PAGE, followed by the transfer to a polyvinylidene fluoride membrane, and stained by colloidal gold (Bio-Rad). The bands were analyzed by peptide mass fingerprinting, as described previously (Fukata et al., 2002). The eluates were also subjected to immunoblotting with anti-coronin-3 (AB15719) antibody.

Coimmunoprecipitation assay

Immunoprecipitation was done as described previously (Kimura et al., 2005). In brief, MIN6 cells were extracted by the addition of L1-buffer (20 mM Tris at pH 7.5, 150 mM NaCl, 1 mM EDTA, 1 µM PMSF, 10 µg/ml leupeptin, 10 µg/ml aprotinin, and 1% NP-40) and then centrifuged at 100,000 ***g*** for 20 minutes at 4°C. The soluble supernatants were incubated with rabbit IgG or anti-Rab27a polyclonal antibody for 6 hours at 4°C. The immunocomplex was then precipitated with protein A Sepharose 4B (GE Healthcare). The bound proteins were eluted using high-salt L1-buffer containing 0.5 M NaCl and were subjected to immunoblotting with anti-Rab27a polyclonal antibody, anti-coronin-3 (ab15719) antibody or anti-coronin-2 antibody, and 0.7% of the total was loaded as input.

Cell culture and transfection

COS-7 cells and MIN6 cells were cultured in Dulbecco's modified Eagle's medium (Sigma-Aldrich) supplemented with 10% and 15% fetal bovine serum, respectively. Lipofectamine 2000 (Invitrogen) reagents were used for transfection according to the manufacturer's instruction.

Protein purification

The fusion proteins GST, GST-Rab27a mutants, GST-Rab3a mutants, GST-SHD, and MBP–coronin-3-ΔC were purified according to the manufacturer's protocol. FLAG-coronin-3 was affinity-purified from transiently expressing COS-7 cell lysates by incubation with anti-FLAG M2 affinity Gel (Sigma-Aldrich) (Kuroda et al., 2002).

Binding assay

Co-transfection of pcDNA-FLAG-Rab mutants and pAcGFP-coronin mutants or pAcGFP-SHD into COS-7 cells was performed as described above. Proteins were solubilized with L2-buffer (20 mM Tris at pH 7.5, 100 mM NaCl, 1 mM EDTA, 1 µM PMSF, 10 µg/ml leupeptin, 10 µg/ml aprotinin, and 0.1% NP-40) at 4°C for 1 hour. FLAG-Rab27a mutants and GFP-coronin-3 mutants were immunoprecipitated with anti-FLAG M2 antibody and anti-GFP antibody, respectively. The immunocomplex was subjected to immunoblotting with anti-GFP antibody or anti-FLAG M2 antibody. In this blot, 0.7% of the total was loaded as input. For direct-binding assay with purified recombinant proteins, the GST-Rab27a mutants coupled with glutathione-Sepharose 4B were prepared as described above. The immobilized beads were incubated with purified FLAG-coronin-3 in L3-buffer (50 mM HEPES at pH 7.5, 150 mM NaCl, 1 µM PMSF, 10 µg/ml leupeptin, 10 µg/ml aprotinin, and 0.1% NP40) for 2 hours at 4°C. The beads were then washed six times with L3-buffer, and suspended with SDS-PAGE sampling buffer. The bound proteins were subjected to immunoblot analysis with anti-GST (GST-2) antibody or anti-FLAG M2 antibody. The in-vitro-binding assays using MBP–coronin-3-ΔC and GST-Rab27a-T23N- or GST-Rab3a-T36N-immobilized beads were carried out the same way.

Immunohistochemistry

Pancreata from male ICR mice (SLC) aged 8-12 weeks were fixed with phosphate-buffered 3% paraformaldehyde and cryosectioned at 5 µm. The tissue sections were subjected to immunostaining. Cryosections of the fixed pancreas were incubated in a mixture of anti-insulin guinea pig antibody (Seikagaku corp.) and anti-Rab27a (M02) monoclonal antibody or anti-coronin-3 antibody, followed by incubation in a mixture of Alexa-Fluor-568 anti-guinea-pig IgG (Molecular Probes) and FITC-conjugated anti-mouse IgG (Vector Laboratories) or FITC-conjugated anti-rabbit IgG (Vector Laboratories).

Pull-down assay

MIN6 cells, pre-incubated with G3-buffer (20 mM HEPES at pH 7.4, 119 mM NaCl, 4.8 mM KCl, 2.5 mM $CaCl_2$, 1.2 mM $MgSO_4$, 1.2 mM KH_2PO_4, 5 mM $NaHCO_3$, 1 mg/ml BSA, and 3 mM glucose), were incubated with G20-buffer (20 mM HEPES at pH 7.4, 119 mM NaCl, 4.8 mM KCl, 2.5 mM $CaCl_2$, 1.2 mM $MgSO_4$, 1.2 mM KH_2PO_4, 5 mM $NaHCO_3$, 1 mg/ml BSA, and 20 mM glucose) for 2 minutes at 37°C. Proteins were solubilized with L4-buffer (50 mM Tris at pH 7.4, 30 mM $MgCl_2$, 10% glycerol, 100 mM NaCl, 1 mM DTT, 1 µM PMSF, 10 µg/ml leupeptin, 10 µg/ml aprotinin, and 0.5% Triton X-100) at 4°C for 5 minutes followed by centrifugation at 100,000 ***g*** for 5 minutes. Then, the supernatants were incubated with GST-SHD- or GST-coronin-3-ΔC-conjugated glutathione-Sepharose 4B beads at 4°C for 30 minutes. The beads were then washed three times with L4-buffer, and suspended with SDS-PAGE sampling buffer (Kondo et al., 2006). The bound proteins were subjected to immunoblot analysis using anti-Rab27a antibody. For binding assay, transfection of pcDNA-T7-Rab27a mutants into COS-7 cells was performed as described above. Proteins were solubilized with L4-buffer at 4°C for 5 minutes followed by centrifugation at 100,000 ***g*** for 5 minutes. The supernatants were then incubated with GST-SHD or GST-coronin-3-ΔC conjugated glutathione-Sepharose 4B beads at 4°C for 30 minutes. Beads were washed three times with L4-buffer and suspended with SDS-PAGE sampling buffer. The bound proteins were subjected to immunoblot analysis using anti-T7 antibody.

siRNA preparation and transfection

A 21-oligonucleotide siRNA duplex was designed as described elsewhere (Elbashir et al., 2001) and was synthesized by RNAi Co., Ltd (Tokyo, Japan) to target the mouse coronin 3 sequence 5′-CAAGACGAGCGCATTTCCAAG-3′. NegaConNaito1 (RNAi Co., Ltd) was used as a negative control.

Live cell imaging

Cells were transfected with plasmid DNA or coronin 3 siRNA using Lipofectamine 2000. After 24 hours of transfection, the cells were analyzed using a confocal laser microscopy system in the consistent presence of 25 mM glucose. At least 30 cells transfected with plasmid DNA or siRNA were examined in each experiment. For FM-4-64-uptake experiments, cells were transfected with plasmid DNA or coronin 3 siRNA by Lipofectamine 2000. At 24 hours after transfection, the cells were incubated for 3 hours in culture medium containing 10 µM FM4-64. They were then thoroughly washed with dye-free medium and used for live imaging. For the analysis of phogrin-GFP internalization and FM4-64 uptake, the rate of cells with cytoplasmic pattern was evaluated. More than 40 randomly selected cells (more than ten cells per experiment) were examined. Data are expressed as the mean ± s.d. from four independent experiments.

Confocal fluorescence microscopy

Images illustrated were acquired using a 63×oil objective (Plan-Apochromat 63×/1.4 Oil DIC; Carl Zeiss). All sections were analyzed with a confocal laser microscopy system (Filters; BP505-530 and LP560, Beam Splitters; HFT488/543 and NFT545, Scan mode; multi track) and software (LSM5 PASCAL; Carl Zeiss) built around an inverted microscope (Axiovert 200M, Carl Zeiss).

Adenovirus production

The FLAG–coronin-3-ΔC expression cassette was excised by digestion with *Swa*I and ligated with the E1-defective adenoviral genome containing cosmid vector (pALC3). The cosmid vector and pMC1-Cre were then co-transfected into 293 cells, with Lipofectamine 2000 reagents were used according to the supplied instructions. Culture medium with the cytopathic effect was harvested and centrifuged to obtain the supernatant fraction. After addition of the supernatant, 293 cells grown at a large scale were cultured for further several days. The cells were then harvested, lysed, and centrifuged at 2000 ***g*** for 10 minutes at 4°C. Amplified adenoviruses in the supernatant fraction were purified with CsCl gradient ultracentrifugation.

Uptake of anti-phogrin antibody

MIN6 cells (6×10^5) were infected with recombinant adenoviruses 40 hours before experiments at a MOI of 100. To label the lumenal domain of phogrin, cells were incubated for 40 minutes at 37°C in the medium containing 25 mM glucose and anti-phogrin antibody (1:100). At the end of the incubation, cells were rinsed in PBS and fixed with 4% PFA, permeabilized with 0.1% Triton X-100, and incubated with Alexa-Fluor-568-conjugated anti-goat antibody (Vo et al., 2004).

We thank Susume Seino, Eji Kawasaki, and Atsushi Shimomura for providing the constructs, Jun-Ichi Miyazaki for providing MIN6 cells, John C. Hutton for providing anti-phogrin antibodies, and Kazuo Toya, Akiko Nakano, Ryusei Nagata, Akiro Satoh, and Shigeki Taniguchi for discussion and help. This work was supported by by KAKENHI (19790636) and Suzuken Memorial Foundation.

References

Appleton, B. A., Wu, P. and Wiesmann, C. (2006). The crystal structure of murine coronin-1: a regulator of actin cytoskeletal dynamics in lymphocytes. *Structure* **14**, 87-96.

Ashcroft, F. M. and Rorsman, P. (2004). Molecular defects in insulin secretion in type-2 diabetes. *Rev. Endocr. Metab. Disord.* **5**, 135-142.

Bahadoran, P., Aberdam, E., Mantoux, F., Busca, R., Bille, K., Yalman, N., de Saint-Basile, G., Casaroli-Marano, R., Ortonne, J. P. and Ballotti, R. (2001). Rab27a: A key to melanosome transport in human melanocytes. *J. Cell Biol.* **152**, 843-850.

Cai, L., Holoweckyj, N., Schaller, M. D. and Bear, J. E. (2005). Phosphorylation of coronin 1B by protein kinase C regulates interaction with Arp2/3 and cell motility. *J. Biol. Chem.* **280**, 31913-31923.

Cheviet, S., Coppola, T., Haynes, L. P., Burgoyne, R. D. and Regazzi, R. (2004). The Rab-binding protein Noc2 is associated with insulin-containing secretory granules and is essential for pancreatic beta-cell exocytosis. *Mol. Endocrinol.* **18**, 117-126.

Elbashir, S. M., Harborth, J., Lendeckel, W., Yalcin, A., Weber, K. and Tuschl, T. (2001). Duplexes of 21-nucleotide RNAs mediate RNA interference in cultured mammalian cells. *Nature* **411**, 494-498.

Engqvist-Goldstein, A. E. and Drubin, D. G. (2003). Actin assembly and endocytosis: from yeast to mammals. *Annu. Rev. Cell Dev. Biol.* **19**, 287-332.

Foger, N., Rangell, L., Danilenko, D. M. and Chan, A. C. (2006). Requirement for coronin 1 in T lymphocyte trafficking and cellular homeostasis. *Science* **313**, 839-842.

Fukata, Y., Itoh, T. J., Kimura, T., Menager, C., Nishimura, T., Shiromizu, T., Watanabe, H., Inagaki, N., Iwamatsu, A., Hotani, H. et al. (2002). CRMP-2 binds to tubulin heterodimers to promote microtubule assembly. *Nat. Cell Biol.* **4**, 583-591.

Fukuda, M. (2005). Versatile role of Rab27 in membrane trafficking: focus on the Rab27 effector families. *J. Biochem.* **137**, 9-16.

Galletta, B. J., Chuang, D. Y. and Cooper, J. A. (2008). Distinct roles for Arp2/3 regulators in actin assembly and endocytosis. *PLoS Biol.* **6**, e1.

Gomi, H., Mizutani, S., Kasai, K., Itohara, S. and Izumi, T. (2005). Granuphilin molecularly docks insulin granules to the fusion machinery. *J. Cell Biol.* **171**, 99-109.

Haddad, E. K., Wu, X., Hammer, J. A., 3rd and Henkart, P. A. (2001). Defective granule exocytosis in Rab27a-deficient lymphocytes from Ashen mice. *J. Cell Biol.* **152**, 835-842.

Hasse, A., Rosentreter, A., Spoerl, Z., Stumpf, M., Noegel, A. A. and Clemen, C. S. (2005). Coronin 3 and its role in murine brain morphogenesis. *Eur. J. Neurosci.* **21**, 1155-1168.

Hume, A. N., Collinson, L. M., Rapak, A., Gomes, A. Q., Hopkins, C. R. and Seabra, M. C. (2001). Rab27a regulates the peripheral distribution of melanosomes in melanocytes. *J. Cell Biol.* **152**, 795-808.

Humphries, C. L., Balcer, H. I., D'Agostino, J. L., Winsor, B., Drubin, D. G., Barnes, G., Andrews, B. J. and Goode, B. L. (2002). Direct regulation of Arp2/3 complex activity and function by the actin binding protein coronin. *J. Cell Biol.* **159**, 993-1004.

Iizaka, M., Han, H. J., Akashi, H., Furukawa, Y., Nakajima, Y., Sugano, S., Ogawa, M. and Nakamura, Y. (2000). Isolation and chromosomal assignment of a novel human gene, CORO1C, homologous to coronin-like actin-binding proteins. *Cytogenet. Cell Genet.* **88**, 221-224.

Itoh, T. and Fukuda, M. (2006). Identification of EPI64 as a GTPase-activating protein specific for Rab27A. *J. Biol. Chem.* **281**, 31823-31831.

Izumi, T., Gomi, H., Kasai, K., Mizutani, S. and Torii, S. (2003). The roles of Rab27 and its effectors in the regulated secretory pathways. *Cell Struct. Funct.* **28**, 465-474.

Kahn, S. E. (2001). Clinical review **135**, The importance of beta-cell failure in the development and progression of type 2 diabetes. *J. Clin. Endocrinol. Metab.* **86**, 4047-4058.

Kasai, K., Ohara-Imaizumi, M., Takahashi, N., Mizutani, S., Zhao, S., Kikuta, T., Kasai, H., Nagamatsu, S., Gomi, H. and Izumi, T. (2005). Rab27a mediates the tight docking of insulin granules onto the plasma membrane during glucose stimulation. *J. Clin. Invest.* **115**, 388-396.

Kimura, T., Watanabe, H., Iwamatsu, A. and Kaibuchi, K. (2005). Tubulin and CRMP-2 complex is transported via Kinesin-1. *J. Neurochem.* **93**, 1371-1382.

Kondo, H., Shirakawa, R., Higashi, T., Kawato, M., Fukuda, M., Kita, T. and Horiuchi, H. (2006). Constitutive GDP/GTP exchange and secretion-dependent GTP hydrolysis activity for Rab27 in platelets. *J. Biol. Chem.* **281**, 28657-28665.

Kotake, K., Ozaki, N., Mizuta, M., Sekiya, S., Inagaki, N. and Seino, S. (1997). Noc2, a putative zinc finger protein involved in exocytosis in endocrine cells. *J. Biol. Chem.* **272**, 29407-29410.

Kuroda, T. S. and Fukuda, M. (2004). Rab27A-binding protein Slp2-a is required for peripheral melanosome distribution and elongated cell shape in melanocytes. *Nat. Cell Biol.* **6**, 1195-1203.

Kuroda, T. S., Fukuda, M., Ariga, H. and Mikoshiba, K. (2002). The Slp homology domain of synaptotagmin-like proteins 1-4 and Slac2 functions as a novel Rab27A binding domain. *J. Biol. Chem.* **277**, 9212-9218.

Machesky, L. M., Reeves, E., Wientjes, F., Mattheyse, F. J., Grogan, A., Totty, N. F., Burlingame, A. L., Hsuan, J. J. and Segal, A. W. (1997). Mammalian actin-related protein 2/3 complex localizes to regions of lamellipodial protrusion and is composed of evolutionarily conserved proteins. *Biochem. J.* **328**, 105-112.

Matsumoto, M., Miki, T., Shibasaki, T., Kawaguchi, M., Shinozaki, H., Nio, J., Saraya, A., Koseki, H., Miyazaki, M., Iwanaga, T. et al. (2004). Noc2 is essential in normal regulation of exocytosis in endocrine and exocrine cells. *Proc. Natl. Acad. Sci. USA* **101**, 8313-8318.

Menasche, G., Pastural, E., Feldmann, J., Certain, S., Ersoy, F., Dupuis, S., Wulffraat, N., Bianchi, D., Fischer, A., Le Deist, F. et al. (2000). Mutations in RAB27A cause Griscelli syndrome associated with haemophagocytic syndrome. *Nat. Genet.* **25**, 173-176.

Nagamatsu, S., Nakamichi, Y., Watanabe, T., Matsushima, S., Yamaguchi, S., Ni, J., Itagaki, E. and Ishida, H. (2001). Localization of cellubrevin-related peptide, endobrevin, in the early endosome in pancreatic beta cells and its physiological function in exo-endocytosis of secretory granules. *J. Cell Sci.* **114**, 219-227.

Nakamura, T., Takeuchi, K., Muraoka, S., Takezoe, H., Takahashi, N. and Mori, N. (1999). A neurally enriched coronin-like protein, ClipinC, is a novel candidate for an actin cytoskeleton-cortical membrane-linking protein. *J. Biol. Chem.* **274**, 13322-13327.

Niki, I., Niwa, T., Yu, W., Budzko, D., Miki, T. and Senda, T. (2003). Ca2+ influx does not trigger glucose-induced traffic of the insulin granules and alteration of their distribution. *Exp. Biol. Med. (Maywood)* **228**, 1218-1226.

Pastural, E., Ersoy, F., Yalman, N., Wulffraat, N., Grillo, E., Ozkinay, F., Tezcan, I., Gedikoglu, G., Philippe, N., Fischer, A. et al. (2000). Two genes are responsible for Griscelli syndrome at the same 15q21 locus. *Genomics* **63**, 299-306.

Pouli, A. E., Emmanouilidou, E., Zhao, C., Wasmeier, C., Hutton, J. C. and Rutter, G. A. (1998). Secretory-granule dynamics visualized in vivo with a phogrin-green fluorescent protein chimaera. *Biochem. J.* **333**, 193-199.

Rosentreter, A., Hofmann, A., Xavier, C. P., Stumpf, M., Noegel, A. A. and Clemen, C. S. (2007). Coronin 3 involvement in F-actin-dependent processes at the cell cortex. *Exp. Cell Res.* **313**, 878-895.

Schafer, D. A. (2002). Coupling actin dynamics and membrane dynamics during endocytosis. *Curr. Opin. Cell Biol.* **14**, 76-81.

Shirane, M. and Nakayama, K. I. (2006). Protrudin induces neurite formation by directional membrane trafficking. *Science* **314**, 818-821.

Spoerl, Z., Stumpf, M., Noegel, A. A. and Hasse, A. (2002). Oligomerization, F-actin interaction, and membrane association of the ubiquitous mammalian coronin 3 are mediated by its carboxyl terminus. *J. Biol. Chem.* **277**, 48858-48867.

Stinchcombe, J. C., Barral, D. C., Mules, E. H., Booth, S., Hume, A. N., Machesky, L. M., Seabra, M. C. and Griffiths, G. M. (2001). Rab27a is required for regulated secretion in cytotoxic T lymphocytes. *J. Cell Biol.* **152**, 825-834.

Takai, Y., Sasaki, T. and Matozaki, T. (2001). Small GTP-binding proteins. *Physiol Rev.* **81**, 153-208.

Taraska, J. W. and Almers, W. (2004). Bilayers merge even when exocytosis is transient. *Proc. Natl. Acad. Sci. USA* **101**, 8780-8785.

Torii, S., Zhao, S., Yi, Z., Takeuchi, T. and Izumi, T. (2002). Granuphilin modulates the exocytosis of secretory granules through interaction with syntaxin 1a. *Mol. Cell. Biol.* **22**, 5518-5526.

Uetrecht, A. C. and Bear, J. E. (2006). Coronins: the return of the crown. *Trends Cell Biol.* **16**, 421-426.

Vitour, D., Lindenbaum, P., Vende, P., Becker, M. M. and Poncet, D. (2004). RoXaN, a novel cellular protein containing TPR, LD, and zinc finger motifs, forms a ternary complex with eukaryotic initiation factor 4G and rotavirus NSP3. *J. Virol.* **78**, 3851-3862.

Vo, Y. P., Hutton, J. C. and Angleson, J. K. (2004). Recycling of the dense-core vesicle membrane protein phogrin in Min6 beta-cells. *Biochem. Biophys. Res. Commun.* **324**, 1004-1010.

Wang, J., Takeuchi, T., Yokota, H. and Izumi, T. (1999). Novel rabphilin-3-like protein associates with insulin-containing granules in pancreatic beta cells. *J. Biol. Chem.* **274**, 28542-28548.

Waselle, L., Coppola, T., Fukuda, M., Iezzi, M., El-Amraoui, A., Petit, C. and Regazzi, R. (2003). Involvement of the Rab27 binding protein Slac2c/MyRIP in insulin exocytosis. *Mol. Biol. Cell* **14**, 4103-4113.

Wennerberg, K., Rossman, K. L. and Der, C. J. (2005). The Ras superfamily at a glance. *J. Cell Sci.* **118**, 843-846.

Wilson, S. M., Yip, R., Swing, D. A., O'Sullivan, T. N., Zhang, Y., Novak, E. K., Swank, R. T., Russell, L. B., Copeland, N. G. and Jenkins, N. A. (2000). A mutation in Rab27a causes the vesicle transport defects observed in ashen mice. *Proc. Natl. Acad. Sci. USA* **97**, 7933-7938.

Yi, Z., Yokota, H., Torii, S., Aoki, T., Hosaka, M., Zhao, S., Takata, K., Takeuchi, T. and Izumi, T. (2002). The Rab27a/granuphilin complex regulates the exocytosis of insulin-containing dense-core granules. *Mol. Cell. Biol.* **22**, 1858-1867.

Zerial, M. and McBride, H. (2001). Rab proteins as membrane organizers. *Nat. Rev. Mol. Cell. Biol.* **2**, 107-117.